NORSAR

ROYAL NORWEGIAN COUNCIL FOR SCIENTIFIC AND INDUSTRIAL RESEARCH

NORSAR Scientific Report No. 1-85/86

FINAL TECHNICAL SUMMARY

1 April - 30 September 1985

L. B. Loughran (ed.)

Kjeller, December 1985

VII.9 NORESS regional event records - wavefield decomposition schemes

The high-quality NORESS recordings of events at local and regional distances exhibit many complex features the significance of which is difficult to assess by visual inspections of the records. What is needed here is fast and robust analyzing schemes for phase-type identification, and estimates of the associated slowness vector. An added advantage would be if the above information or part of it can be used for time-domain filtering of the original records so as to visually expose major features. The ability to extract significantly more information from local and regional event records is essential for more advanced seismogram analysis like forward and inverse modelling and not at least expert system designs. In this context we have conducted a practical analysis experiment on NORESS records of local and regional events, using different techniques, namely, f-k, semblance and the novel 3-comp. analysis technique described in subsection VII.8.

f-k analysis

Our interest here is to have a computationally fast, sliding window approach, and the necessary details here are as follows: Consider an array of N-sensors whose locations are r_j; j=1,N. For a prespecified time window of the records, the respective Fourier transforms are $C_j(\omega)$. The corresponding frequency-wavenumber (f-k) spectrum is defined as

$$P(\omega,\bar{k}) = \sum_{j=1}^{N} \sum_{l=1}^{N} S_{jl}(\omega) \exp(i\bar{k}(\bar{r}_j-\bar{r}_l)) \qquad (1)$$

where S_{jl} is the cross-spectrum between the j-th and l-th instruments. Sinc $S_{jl}(\omega) = C_j(\omega) \cdot C_l(\omega)$, eq. (1) may be rewritten as

$$P(\omega,\bar{k}) = \sum_{j=1}^{N} \sum_{l=1}^{N} C_j(\omega) C_l^*(\omega) \exp i(\bar{k}\cdot\bar{r}_j) \exp -i(\bar{k}\cdot\bar{r}_l)$$

$$= \sum_{j=1}^{N} C_j(\omega) \exp i(\bar{k}\cdot\bar{r}_j) \cdot \sum_{l=1}^{N} C_l^*(\omega) \cdot [\exp i(\bar{k}\cdot\bar{r}_l)]$$

$$= \left| \sum_{j=1}^{N} C_j(\omega) \exp i(\bar{k}\cdot\bar{r}_j) \right|^2$$

which only involves a single summation. This technique for $P(\omega,k)$-estimation was first proposed by Flinn and Smart (1971). Additional speed-up in programming is obtained by using properties of the exponential function to eliminate indexing during power component summation and by using the "sum of angles" formula for sine and cosine terms when estimating the Fourier spectrum $C_j(\omega)$. Frequency domain smoothing was performed by a Hanning operation, i.e., replacing $C_j(\omega)$ by

$$\frac{1}{4} C_j(\omega_1) + \frac{1}{2} C_j(\omega) + \frac{1}{4} C_j(\omega_2)$$

ω_1, ω_2 being $\omega \pm .5$ Hz) during the initial spectrum estimation.

Comments: f-k analysis, including its ML variants, is generally not rated a robust analyzing technique for several reasons. In ML estimation the signal is presumed non-stochastic, which is not necessarily the case in shorter time windows, while for conventional f-k relatively long time windows are needed ($T > 1.6$ sec) to ensure a good Fourier spectrum estimate. Perhaps the most intriguing aspect of f-k analysis is that in most applications, the slowness estimate extracted is tied to peak power in the f-k space. Under adverse conditions with interfering wavelets, peak power is not always associated with the "primary" phase and thus wild slowness estimates may ensure. Let us add that under more normal conditions, conventional f-k analysis represents in many respects a convenient tool for seismogram decomposition.

Semblance

So-called semblance analysis is in many respects similar to VESPAGRAM analysis, and as such is of potential interest in processing of regional NORESS records. The semblance parameter S_t, essentially the normalized beam power over a given window $2\Delta T$ and for a given slowness, is defined as:

$$S_t = \frac{\sum_{p=t-\Delta T}^{t+\Delta T} \left(\sum_{i=1}^{N} x(p)_i \right)^2}{N \sum_{p=t-\Delta T}^{t+\Delta T} \left(\sum_{i=1}^{N} x(p)_i \right)^2} \qquad (3)$$

The S_t parameter is a simple signal coherency measure which appears to provide reasonable phase velocity estimates even for complex local and regional event records. Besides its calculational simplicity, an added advantage is that the semblance technique works well even for short time windows of the order of .5

sec. In practical use the looping over the P and S crustal velocity window, say 3-10 kms^{-1} for a given azimuth and signal window width. We may also loop over azimuth for obtaining a more refined velocity-azimuth estimate for dominant phases in the record.

3-comp. signal analysis

The theoretical basis for this technique is described in subsection VII.8, so here we will only comment on the practical usage of this technique. The output from the 3-comp. analysis (single site) is probability of P, S-, Rayleigh and Love-waves in the records as a function of time and azimuth. Since this technique embodies the estimation of the principal axis of the particle motion ellipsoid, it is easy to estimate also the apparent angle of incidence for an incoming phase. This parameter can in turn be converted to apparent velocity and henceforth epicentral distance via standard travel time tables. The error in the corresponding azimuth and velocity estimates are of the order of ± 15 deg and ± 3 kms^{-1}. Important, most of the observed deviations are deterministic, that is, due to structural effects and thus to a large extent can be removed by appropriate corrections in the same way as done for arrays.

The advantages with the novel 3-comp. analysis is that it provides an efficient means for decomposition of even complex wavetrains, can operate on short time windows of the order of 0.5-1.0 sec and provides good estimates of the slowness vector. A drawback is easy triggering on noise wavelets which we consider removable by appropriate filtering schemes.

Practical examples:

The relative merits of the 3 analysis methods discussed above have been tested on real data and detailed results for a presumed explosion near Leningrad (Date: 29 Jan 85; OT: 11.59.47; Lat. & Long.: 59.3N, 28.1E) are presented below in Figs. VII.9.1-6 and Tables VII.9.1-3.

All the figures have the same time scale and thus are easily comparable. The main features are summarized in the figure captions.

In Tables VII.9.1-3 the outputs from f-k, semblance and 3-comp. analysis are presented in detail. All three methods give reasonable velocity and azimuth estimates of the first part of the P-wave train (centered around t = 126 sec), although the semblance results by far appear to be the most robust ones. Interestingly, the single 3-comp. station analysis results contain all principal phase information features as found in the semblance and f-k results plus some more, most of which is termed coda signature of the event in question. Also, the 3-comp. analysis results are rather stable when based on beam traces formed from the 4 NORESS stations in question. For the shear wave section we have not run the Love and Rayleigh models of our 3-comp. analysis package.

Comments: The results presented are rather self-evident, so we will only remark that the advantage of f-k is scanning of the whole "space", but that in more extreme cases the associated (peak power) slowness estimate could be very wrong. Semblance is robust and provides adequate slowness estimates, but for easy use in an automated mode require *a priori* information on azimuth. Furthermore, semblance function values are convenient for generating weighting filters in the same way as used in 3-comp. analysis (Fig. VII.9.5). Finally, the 3-comp. results do not compare unfavorably with those obtained from f-k and semblance analysis using whole array recordings. It also seems to work well for signals with poor SNR as demonstrated elsewhere.

T. Egilson
E.S. Husebye
B.O. Ruud

References

Flinn, E.S. & E. Smart (1971): Fast frequency-wavenumber analysis and Fisher signal detection in real-time infrasonic array data processing, Geophys. J.R. Astr. Soc., 26, 279-284.

ANALYSIS FREQUENCY : 3.2

WINDOWS :		1.00			1.50			2.00	
TIME	POWER	AZIM	VELO	POWER	AZIM	VELO	POWER	AZIM	VELO
120.00	39.3	0.73	6.15	40.6	0.73	6.15	42.6	240.95	47.20
120.50	36.7	83.75	10.40	37.1	86.01	11.27	37.1	263.16	19.30
121.00	38.1	126.47	16.79	39.2	103.57	16.29	41.8	292.38	26.43
121.50	36.7	225.72	4.30	37.9	225.73	4.41	44.3	188.13	13.75
122.00	37.2	228.95	11.82	39.5	222.80	13.21	42.7	232.59	22.71
122.50	34.7	221.82	19.06	32.3	1.74	14.72	41.3	131.13	4.63
123.00	34.6	250.18	11.06	36.4	259.99	9.38	37.9	129.45	4.75
123.50	38.2	78.59	19.06	38.7	120.96	27.78	38.5	234.46	18.83
124.00	39.2	147.53	37.27	39.8	201.04	34.89	43.9	225.00	18.09
124.50	36.6	245.73	8.69	36.2	133.51	4.46	53.2	83.05	11.77
125.00	37.2	265.26	14.21	37.2	102.99	12.14	56.4	78.69	10.59
125.50	32.8	299.05	9.44	33.3	110.10	11.13	55.8	80.75	11.16
126.00	51.9	80.31	11.68	51.0	77.62	11.58	57.0	76.33	12.76
126.50	56.3	83.66	10.73	55.7	81.16	10.67	59.6	78.69	10.59
127.00	56.3	80.75	11.16	56.2	83.37	11.23	56.2	76.26	10.49
127.50	53.7	77.01	12.14	53.4	79.82	12.27	55.2	74.25	11.99
128.00	51.5	75.65	10.95	51.2	75.65	10.95	52.6	69.30	10.10
128.50	41.9	292.56	6.90	42.2	291.64	7.17	44.9	294.59	7.49
129.00	43.0	231.01	6.00	42.0	231.88	5.68	50.0	99.16	15.48
129.50	42.0	90.78	6.66	43.1	90.78	6.66	48.2	124.88	12.08
130.00	42.0	162.76	16.01	43.6	145.62	21.11	49.0	156.25	17.79
130.50	46.2	83.66	10.73	45.5	83.37	11.23	48.4	86.88	8.82
131.00	44.8	107.78	8.73	44.9	109.13	9.37	47.2	123.16	5.42
131.50	43.1	88.45	13.13	43.7	88.45	13.13	44.2	74.36	18.72
132.00	44.5	81.87	13.75	43.4	79.29	12.91	47.5	96.34	17.89
132.50	42.1	125.54	18.83	43.9	119.48	18.40	46.9	86.63	28.54
133.00	43.8	84.17	9.87	44.3	86.19	10.78	51.5	78.69	10.59
133.50	41.0	83.85	7.43	41.4	86.99	8.51	47.0	76.70	8.60
134.00	40.6	81.53	10.23	38.5	76.83	10.07	45.5	80.36	9.04
134.50	45.3	79.16	10.16	45.7	79.16	10.16	49.4	84.99	8.49
135.00	41.7	78.18	11.06	41.9	71.57	11.82	43.9	330.52	18.40
135.50	41.8	86.99	8.51	41.1	84.99	8.49	44.3	85.86	7.03
136.00	42.9	102.77	6.32	43.1	104.89	5.95	47.2	168.69	95.31
136.50	43.1	50.44	16.29	43.1	47.39	14.31	45.5	141.71	20.08
137.00	38.6	92.17	6.15	39.0	135.00	11.09	45.7	90.88	7.48
137.50	43.2	107.78	8.73	43.3	111.19	9.25	45.8	109.06	8.35
138.00	44.6	71.57	17.08	45.3	77.28	15.29	50.7	98.84	10.67
138.50	43.9	105.46	9.97	44.3	109.23	10.67	45.0	88.92	9.17
139.00	39.7	120.96	27.78	41.3	130.91	24.48	44.2	103.67	12.76
139.50	40.7	118.50	12.26	39.0	137.39	14.31	40.6	155.92	9.44
140.00	39.0	94.64	13.09	38.5	107.45	13.25	48.4	135.00	68.73
140.50	37.3	92.64	7.47	39.3	240.95	47.20	39.5	42.40	5.20
141.00	41.4	100.98	7.12	41.1	103.47	6.66	43.7	78.69	7.33
141.50	41.4	132.92	6.24	41.3	128.95	5.18	43.2	117.47	17.25
142.00	38.6	123.86	5.11	38.5	125.81	4.99	47.1	106.43	153.69
142.50	40.5	304.00	9.37	39.7	261.87	68.73	46.4	84.81	8.80
143.00	43.3	135.00	10.41	42.7	133.32	10.10	45.0	113.55	11.42
143.50	40.1	72.05	6.51	38.9	71.10	6.30	42.5	71.57	153.69
144.00	42.1	258.02	14.41	42.5	253.81	15.06	43.4	274.18	11.92
144.50	43.7	102.72	15.29	44.3	102.72	15.29	44.5	120.38	14.46
145.00	42.8	55.30	30.74	42.5	346.61	22.51	46.2	306.57	12.59
145.50	41.4	152.35	20.50	41.4	138.18	19.06	47.1	115.56	19.06
146.00	41.3	107.05	6.20	41.1	107.05	6.20	45.7	164.74	14.21
146.50	39.9	104.24	7.03	38.3	107.56	5.87	40.3	246.16	10.34
147.00	39.3	59.38	8.54	40.7	59.04	9.26	40.1	262.48	9.09
147.50	39.0	260.31	11.68	39.6	266.19	10.78	41.4	106.05	6.40
148.00	40.5	207.35	14.89	41.7	218.42	13.13	43.0	220.49	9.02
148.50	38.8	16.23	5.91	39.9	16.23	5.91	48.0	109.00	7.53
149.00	39.3	243.43	10.51	40.4	246.45	11.42	45.5	69.78	24.00
149.50	39.2	227.96	5.92	40.3	225.99	5.92	43.5	69.90	11.13
150.00	46.3	105.57	7.67	45.7	108.43	7.32	45.7	108.43	7.32

Table VII.9.1a Output of "sliding" window f-k analysis for signal "center" frequency f_0=3.2 Hz and whole NORESS array except A-ring. Three different window lengths are used, namely: 1.0, 1.5 and 2.0 sec. Other values of f_0 gave less consistent results vis-à-vis "true" velocity and azimuth at 8.38 kms^{-1} and 92.60 deg. A comparison with semblance results in Table VII.9.2 clearly implies why semblance is termed a robust analysis technique re f-k.

FK-ANALYSIS WITH SLIDING TIMEWINDOW

DATA FILE : NRS85029 11594002

ANALYSED FREQUENCY : 3.20

WINDOWS :		1.50			2.00			2.50	
TIME	POWER	AZIM	VELO	POWER	AZIM	VELO	POWER	AZIM	VELO
210.00	38.1	99.34	3.04	40.6	0.91	3.86	42.6	3.24	4.58
210.50	37.7	74.36	9.36	41.2	131.13	2.32	45.8	55.62	10.56
211.00	38.3	225.00	5.93	43.0	111.57	5.26	47.7	107.45	6.62
211.50	41.0	101.82	5.53	45.1	105.02	5.72	47.4	96.63	5.61
212.00	36.7	311.70	3.30	40.9	79.51	8.85	46.2	112.01	4.79
212.50	40.1	87.71	9.71	46.3	115.02	4.89	49.5	112.89	4.97
213.00	38.6	87.88	8.99	45.0	96.84	9.65	48.9	109.54	7.39
213.50	37.9	20.22	12.00	45.0	102.99	6.07	48.0	105.26	7.10
214.00	42.1	112.39	4.97	42.3	337.83	8.33	42.9	336.25	8.90
214.50	39.1	130.43	6.85	41.7	137.60	7.80	43.0	137.60	7.80
215.00	44.1	107.45	6.62	43.7	114.15	7.65	44.0	234.95	2.97
215.50	37.5	136.51	4.52	42.0	113.75	8.90	47.7	96.34	3.85
216.00	36.8	239.04	13.89	42.2	91.40	5.93	45.4	88.15	7.83
216.50	41.0	135.00	10.11	40.9	95.60	4.74	49.0	113.20	4.56
217.00	40.2	94.84	4.10	48.3	106.11	5.19	51.3	109.39	4.86
217.50	43.7	91.98	9.37	49.0	108.43	76.84	50.4	120.96	3.79
218.00	39.9	306.25	13.06	44.9	106.56	6.30	46.8	260.10	3.80
218.50	44.1	112.89	4.97	46.2	93.37	14.27	47.2	90.83	3.52
219.00	46.3	121.91	3.89	45.8	117.90	4.21	49.9	124.56	4.45
219.50	42.5	125.38	2.87	49.8	85.81	5.91	54.1	121.29	4.07
220.00	43.7	111.97	3.95	45.6	128.48	4.88	52.6	126.12	5.31
220.50	46.9	86.99	12.77	48.8	121.87	5.58	49.9	3.62	3.07
221.00	44.6	60.95	7.37	50.8	83.66	5.37	50.6	75.76	3.52
221.50	50.5	120.17	4.89	50.4	115.14	4.49	55.4	107.02	4.74
222.00	46.9	122.47	6.21	52.9	97.82	4.72	52.3	120.53	5.37
222.50	49.9	74.54	4.96	53.9	77.01	6.07	53.9	112.01	4.79
223.00	46.5	343.18	5.41	49.0	343.44	6.30	50.8	127.23	2.56
223.50	50.4	77.62	5.79	53.0	67.49	5.47	53.4	71.57	5.12
224.00	48.2	111.57	5.26	47.8	120.96	41.67	51.2	348.98	3.10
224.50	44.5	50.44	8.15	45.0	40.24	4.76	51.0	88.73	5.40
225.00	47.3	132.14	2.86	50.1	96.63	5.61	53.0	100.18	6.13
225.50	47.2	100.01	4.69	50.6	68.81	4.62	52.3	93.37	4.75
226.00	43.5	185.33	3.23	48.7	126.51	2.54	49.9	128.75	2.59
226.50	46.4	86.76	4.58	51.5	81.33	4.07	55.0	76.22	4.45
227.00	47.9	94.64	6.55	50.4	96.13	6.87	52.4	99.06	3.48
227.50	42.6	65.92	4.72	46.2	269.29	3.00	52.5	267.88	3.00
228.00	43.7	64.75	4.15	52.3	73.39	4.09	53.4	71.57	4.04
228.50	48.6	67.11	4.97	46.9	61.99	4.56	46.4	152.10	12.63
229.00	42.9	269.29	3.00	47.5	189.32	3.58	49.5	168.81	3.38
229.50	48.8	95.55	3.96	50.5	72.91	4.11	51.8	68.96	17.45
230.00	44.7	169.99	14.08	43.2	165.47	8.71	47.2	118.01	4.56
230.50	40.6	72.98	4.74	47.4	76.83	5.03	53.7	93.37	4.76
231.00	43.0	123.41	4.32	48.3	97.82	4.72	48.7	340.06	3.31
231.50	41.0	135.92	2.77	44.9	99.69	5.84	52.2	96.63	5.61
232.00	44.3	91.17	4.96	51.9	88.73	5.40	52.6	86.76	4.53
232.50	48.5	100.84	5.08	49.8	118.20	3.10	52.6	117.53	3.04
233.00	44.2	101.31	5.30	51.5	98.84	5.34	48.5	209.65	3.25
233.50	46.5	98.84	5.34	44.7	8.13	34.37	47.5	116.18	3.70
234.00	47.3	115.97	5.60	46.7	279.90	3.80	54.6	91.12	4.76
234.50	49.5	91.47	5.23	47.2	258.18	5.53	56.0	93.37	4.76
235.00	40.0	84.81	7.33	54.7	93.99	5.64	57.1	107.59	5.65
235.50	45.9	65.88	4.41	49.7	117.35	7.44	51.1	118.50	5.10
236.00	49.8	91.22	5.17	51.4	114.68	5.97	56.6	120.53	5.37
236.50	53.9	91.12	4.76	55.3	119.05	4.72	59.4	101.73	4.49
237.00	46.6	120.38	7.23	53.6	107.70	4.93	56.8	107.76	4.37
237.50	46.1	146.04	4.11	48.6	144.04	3.86	53.2	144.04	3.86
238.00	48.7	121.66	4.40	48.0	216.12	5.31	50.2	28.74	6.87
238.50	51.4	100.41	4.88	50.5	96.07	5.14	50.9	329.47	5.37
239.00	46.2	77.15	4.16	50.2	326.77	7.01	50.2	326.77	7.01
239.50	50.8	91.17	4.96	50.8	91.17	4.96	50.8	91.17	4.96
240.00	45.4	28.50	6.10	45.4	28.50	6.10	45.4	28.50	6.10

Table VII.9.1b Output of "sliding" window f-k analysis for shear wave section, caption otherwise as for a).

FILTER : 3
AZIMUTH : 90.00

WINDOW :	0.50		1.00		1.50	
TIME	SEMBL	VELO	SEMBL	VELO	SEMBL	VELO
120.00	0.07	13.00	0.07	13.75	0.09	13.75
120.50	0.16	12.25	0.13	12.75	0.12	12.75
121.00	0.19	12.75	0.19	12.25	0.14	12.25
121.50	0.10	10.50	0.08	13.00	0.10	12.75
122.00	0.13	6.00	0.10	6.25	0.08	6.25
122.50	0.07	12.75	0.07	7.00	0.08	6.50
123.00	0.07	7.00	0.08	13.75	0.11	12.75
123.50	0.19	13.75	0.12	13.75	0.10	6.75
124.00	0.17	6.75	0.11	6.75	0.10	13.75
124.50	0.09	11.00	0.12	6.75	0.12	6.75
125.00	0.15	6.00	0.19	8.75	0.16	8.75
125.50	0.28	8.75	0.23	9.25	0.39	9.25
126.00	0.49	11.00	0.71	9.25	0.75	9.25
126.50	0.82	9.25	0.80	9.25	0.79	9.25
127.00	0.82	9.25	0.79	9.25	0.79	9.25
127.50	0.76	9.75	0.75	9.75	0.72	9.25
128.00	0.55	10.75	0.62	10.00	0.64	10.00
128.50	0.50	9.25	0.45	9.25	0.48	10.75
129.00	0.30	13.00	0.22	13.00	0.36	9.25
129.50	0.33	7.50	0.24	7.50	0.20	8.75
130.00	0.13	6.50	0.31	7.50	0.29	8.75
130.50	0.47	10.75	0.35	10.75	0.34	8.75
131.00	0.43	8.00	0.44	8.75	0.39	8.75
131.50	0.31	8.50	0.39	8.50	0.40	8.75
132.00	0.44	8.75	0.34	8.75	0.31	8.75
132.50	0.12	13.25	0.25	11.00	0.27	11.00
133.00	0.22	11.00	0.23	9.75	0.19	8.75
133.50	0.29	7.50	0.26	8.75	0.24	8.25
134.00	0.28	7.25	0.24	7.25	0.30	9.75
134.50	0.44	13.00	0.51	9.75	0.45	9.75
135.00	0.63	9.25	0.55	9.25	0.47	9.25
135.50	0.18	7.50	0.31	8.00	0.40	9.25
136.00	0.30	7.00	0.24	7.00	0.21	7.00
136.50	0.14	7.00	0.15	7.00	0.16	7.00
137.00	0.10	9.75	0.10	7.50	0.14	8.50
137.50	0.28	8.50	0.23	8.50	0.18	8.75
138.00	0.23	7.50	0.25	7.50	0.27	7.50
138.50	0.29	7.50	0.32	7.50	0.29	7.50
139.00	0.34	8.00	0.32	8.00	0.29	8.00
139.50	0.25	7.25	0.27	8.25	0.30	8.25
140.00	0.34	8.25	0.28	8.00	0.25	8.25
140.50	0.19	8.75	0.25	8.00	0.27	8.00
141.00	0.36	7.00	0.26	7.00	0.19	6.50
141.50	0.13	6.50	0.12	6.50	0.14	6.50
142.00	0.09	13.75	0.08	13.75	0.10	8.00
142.50	0.16	12.75	0.15	12.75	0.11	8.00
143.00	0.18	8.75	0.14	7.25	0.17	7.25
143.50	0.22	7.25	0.17	7.25	0.18	7.25
144.00	0.12	6.00	0.25	9.75	0.22	9.25
144.50	0.34	12.00	0.33	12.25	0.30	12.25
145.00	0.36	12.25	0.30	12.25	0.29	12.25
145.50	0.13	11.00	0.20	11.00	0.22	11.00
146.00	0.20	8.00	0.11	8.00	0.10	8.00
146.50	0.05	6.25	0.13	8.00	0.16	9.25
147.00	0.29	9.25	0.21	9.25	0.20	8.75
147.50	0.32	8.75	0.28	8.00	0.27	9.00
148.00	0.24	8.50	0.26	9.00	0.23	9.00
148.50	0.09	6.25	0.11	9.00	0.14	9.00
149.00	0.05	9.00	0.04	6.25	0.07	6.25
149.50	0.14	7.00	0.20	8.00	0.24	8.00
150.00	0.40	8.00	0.43	8.00	0.37	8.00

Table VII.9.2a Output of "sliding" window semblance analysis with azimuth fixed at 90 deg, and traces 3.0-5.0 Hz bandpass filtered. Windows of lengths 0.5, 1.0 and 1.5 have been used. Semblance values less than 0.3 not considered significant. Finally, fixing azimuths at 80 and 100 deg did not profoundly change the semblance results displayed here.

SEMBLANCE COHERENCY ANALYSIS OF NORESS SPZ DATA.
DATA FILE :NRS85029 11594002
CHANNELS NOT USED : B3 B4 B5 A1 A2 A3 B1 B2

FILTER : 2
AZIMUTH : 90.00

WINDOW :	1.00		1.50		2.00	
TIME	SEMBL	VELO	SEMBL	VELO	SEMBL	VELO
210.00	0.35	7.50	0.32	7.50	0.28	7.50
210.50	0.25	7.50	0.31	7.50	0.28	7.50
211.00	0.20	7.25	0.19	7.50	0.18	7.50
211.50	0.11	7.50	0.12	3.50	0.15	7.25
212.00	0.20	4.00	0.17	4.00	0.16	3.75
212.50	0.24	4.00	0.19	4.00	0.16	4.00
213.00	0.16	7.00	0.16	7.25	0.18	4.25
213.50	0.19	5.50	0.15	5.50	0.15	5.25
214.00	0.17	5.50	0.17	5.50	0.17	5.50
214.50	0.15	5.25	0.18	5.25	0.19	6.50
215.00	0.25	6.75	0.23	6.75	0.20	6.75
215.50	0.25	6.75	0.25	6.75	0.23	6.75
216.00	0.20	6.75	0.23	6.75	0.19	6.75
216.50	0.23	4.25	0.21	4.25	0.20	4.25
217.00	0.28	4.25	0.33	4.25	0.29	4.25
217.50	0.33	4.25	0.30	4.25	0.24	4.25
218.00	0.19	4.00	0.20	4.00	0.22	5.00
218.50	0.20	6.00	0.20	5.00	0.20	5.00
219.00	0.23	5.00	0.21	5.00	0.19	7.00
219.50	0.19	7.00	0.22	6.25	0.19	5.00
220.00	0.18	6.25	0.19	7.00	0.17	7.50
220.50	0.16	3.25	0.15	6.00	0.20	5.75
221.00	0.22	5.75	0.18	5.75	0.16	5.75
221.50	0.17	5.75	0.16	5.75	0.16	5.75
222.00	0.13	6.75	0.15	5.50	0.17	4.75
222.50	0.19	4.00	0.14	3.75	0.15	4.00
223.00	0.21	4.00	0.24	4.25	0.27	4.25
223.50	0.33	4.25	0.31	4.25	0.29	4.50
224.00	0.35	4.50	0.35	4.50	0.30	4.50
224.50	0.27	5.00	0.27	4.50	0.27	4.50
225.00	0.16	3.00	0.17	3.00	0.22	4.50
225.50	0.17	4.50	0.18	4.25	0.21	4.25
226.00	0.32	5.00	0.28	4.25	0.23	4.25
226.50	0.30	4.25	0.34	5.00	0.31	5.00
227.00	0.29	5.00	0.29	5.00	0.26	5.00
227.50	0.26	5.25	0.21	5.50	0.20	5.00
228.00	0.15	3.00	0.13	3.25	0.14	5.25
228.50	0.17	3.50	0.18	3.50	0.18	3.50
229.00	0.22	3.50	0.21	3.50	0.23	3.75
229.50	0.29	3.75	0.26	3.75	0.23	3.75
230.00	0.25	4.00	0.21	3.75	0.20	3.75
230.50	0.09	3.50	0.17	3.75	0.17	3.75
231.00	0.07	3.00	0.07	7.50	0.08	7.50
231.50	0.11	7.50	0.09	7.50	0.12	4.50
232.00	0.19	4.50	0.22	4.50	0.20	4.50
232.50	0.30	4.50	0.24	4.50	0.22	4.50
233.00	0.23	4.50	0.30	4.50	0.31	4.50
233.50	0.34	4.25	0.28	4.25	0.33	4.50
234.00	0.41	4.25	0.46	4.25	0.43	4.75
234.50	0.48	4.75	0.44	4.75	0.46	4.75
235.00	0.51	4.75	0.47	4.75	0.44	4.75
235.50	0.41	4.75	0.50	4.75	0.52	4.75
236.00	0.54	4.75	0.56	4.50	0.53	4.50
236.50	0.60	4.50	0.51	4.50	0.44	4.50
237.00	0.38	4.50	0.36	4.50	0.38	4.50
237.50	0.11	7.00	0.14	5.25	0.23	4.50
238.00	0.07	3.00	0.12	4.50	0.15	4.50
238.50	0.22	4.00	0.21	4.25	0.19	4.25
239.00	0.34	4.25	0.29	4.25	0.28	4.50
239.50	0.38	4.50	0.36	4.50	0.35	4.50
240.00	0.38	4.50	0.30	4.50	0.06	3.00

Table VII.9.2b Output of "sliding" window semblance analysis for shear wave section. Caption otherwise as for a).

RELATION OF APPARENT PHASE VELOCITY AND SLOWNESS FOR
AZIMUTHS OF MAXIMUM PROBABILITY WITHIN EACH TIMEWINDOW

TIME	PROBABILITY	AZIMUTH	VELOCITY
120.00	0.28		
120.50	0.01		
121.00	0.00		
121.50	0.58	0.00	10.473
122.00	0.98	14.00	8.399
122.50	0.34	0.00	6.000
123.00	0.45	164.00	6.000
123.50	0.00		
124.00	0.21		
124.50	0.79	24.00	8.281
125.00	0.92	10.00	8.632
125.50	0.20		
126.00	0.62	62.00	10.501
126.50	0.57	86.00	10.994
127.00	0.79	90.00	12.190
127.50	1.00	98.00	14.423
128.00	0.74	94.00	15.192
128.50	0.09		
129.00	0.90	36.00	19.155
129.50	0.56	44.00	17.023
130.00	0.77	74.00	9.902
130.50	0.87	62.00	11.351
131.00	0.76	76.00	28.976
131.50	0.55	172.00	100.000
132.00	0.02		
132.50	0.04		
133.00	0.62	118.00	6.000
133.50	0.52	66.00	6.000
134.00	0.95	70.00	6.151
134.50	0.97	158.00	11.394
135.00	0.41	132.00	10.515
135.50	0.09		
136.00	0.00		
136.50	0.00		
137.00	0.06		
137.50	0.05		
138.00	0.00		
138.50	0.00		
139.00	0.56	98.00	20.071
139.50	0.51	122.00	7.057
140.00	0.33	114.00	6.000
140.50	0.72	112.00	6.000
141.00	0.72	142.00	6.815
141.50	0.49	74.00	8.861
142.00	0.57	118.00	7.368
142.50	0.18		
143.00	0.68	92.00	7.063
143.50	0.84	164.00	18.327
144.00	0.71	162.00	6.573
144.50	0.71	92.00	14.904
145.00	0.18		
145.50	0.47	180.00	9.164
146.00	0.82	38.00	6.620
146.50	0.15		
147.00	0.07		
147.50	0.68	30.00	10.593
148.00	0.76	110.00	6.162
148.50	0.47	52.00	8.255
149.00	0.63	14.00	6.867
149.50	0.78	104.00	11.011
150.00	0.47	118.00	6.948

Table VII.9.3a Estimates of apparent P-wave velocity at site A_0 on the basis of the 3-comp. seismogram analysis. Window length 1.0 sec and traces 3.0-5.0 Hz bandpass filtered. For P-wave presences, probabilities less than 30 per cent (0.3), velocity estimates deleted due to lack of significance.

PRINTING OF APPARENT PHASE VELOCITY AND SLOWNESS FOR
AZIMUTHS OF MAXIMUM PROBABILITY WITHIN EACH TIMEWINDOW

TIME	PROBABILITY	AZIMUTH	VELOCITY	SLOWNESS
210.00	0.39	122.00	10.803	10.292
210.50	0.01			
211.00	0.01			
211.50	0.00			
212.00	0.00			
212.50	0.00			
213.00	0.00			
213.50	0.50	180.00	10.143	10.962
214.00	0.17			
214.50	0.15			
215.00	0.01			
215.50	0.04			
216.00	0.12			
216.50	0.63	180.00	3.464	32.098
217.00	1.00	180.00	3.613	30.775
217.50	0.04			
218.00	0.98	128.00	5.717	19.451
218.50	0.10			
219.00	0.03			
219.50	0.05			
220.00	0.12			
220.50	0.40	110.00	3.464	32.098
221.00	0.83	116.00	3.464	32.098
221.50	0.00			
222.00	0.00			
222.50	0.76	150.00	3.464	32.098
223.00	0.32	122.00	4.317	25.759
223.50	0.20			
224.00	0.00			
224.50	0.01			
225.00	0.00			
225.50	0.02			
226.00	0.48	146.00	3.671	30.292
226.50	0.23			
227.00	0.93	116.00	3.629	30.643
227.50	0.50	92.00	3.666	30.328
228.00	0.78	70.00	3.612	30.784
228.50	0.79	74.00	3.966	28.036
229.00	0.63	26.00	9.527	11.671
229.50	0.22			
230.00	0.00			
230.50	0.04			
231.00	0.55	0.00	3.464	32.098
231.50	0.02			
232.00	0.08			
232.50	0.04			
233.00	0.66	26.00	3.464	32.098
233.50	0.66	14.00	3.619	30.726
234.00	0.40	0.00	3.883	28.637
234.50	0.02			
235.00	0.14			
235.50	0.00			
236.00	0.00			
236.50	0.00			
237.00	0.00			
237.50	0.06			
238.00	0.84	64.00	3.543	31.383
238.50	0.59	72.00	5.546	20.050
239.00	0.16			
239.50	0.26			
240.00	0.56	30.00	3.464	32.098

Table VII.9.3b Estimate of apparent shear wave analysis for shear wave section; caption otherwise as for a).

Figure captions

Fig. VII.9.1: Filtered 3-comp. traces for station A0; the z-component is representative for the other NORESS stations. a) P-wave section, filter 3.0-5.0 Hz; b) shear wave section, filter 2.0-4.0 Hz.

Fig. VII.9.2a): P-wave semblance estimates as a function of time and phase velocity for T = 1.0 sec.; azimuth 90°. b) Same as a) except that looping is over azimuth with vel = 9.0 kms^{-1}. For details see Table VII.9.2a.

Fig. VII.9.3a): Shear wave semblance estimates as a function of time and phase velocity for T = 1.0 sec; azimuth 90°. b) Same as a) except that looping is over azimuth with vel 4.5 kms^{-1}. For details see Table VII.9.2b.

Fig. VII.9.4a): 3-component analysis, P-wave probabilities (0.9 ≡ 90%) as a function of time and azimuth; window T = 1.0 sec. b) Same as for a) except this time for the shear wave section. For estimates of apparent velocities, see Table VII.9.3.

Fig. VII.9.5a: Probability filtered records; only that part of the seisaogram having probabilities of being P-wave motion within the azimuth sector 90 ± 30° is retained. b) Probability filtered shear wave section.

Fig. VII.9.6a-e): This sequence of figures demonstrates the viability of 3-comp. signal analysis under adverse conditions, i.e., SNR around 1 or less. a) Filtered P-wave section (3.0-5.0 Hz) for the beam formed on the basis of the 4 NORESS 3-comp. stations; b) The probability filtered variant of a); c) Unfiltered beam record; d) The probability filtered variant of c) (the original non-band pass record); e) Band pass filtering of the d)-records, which should be compared to b). Our remark is that this record sequence demonstrates convincingly that the 3-comp. analyzing technique works well for SNR around 1 or even smaller values. It should be added that we were unable to reproduce a counterpart to e) on the basis of a single station 3-comp. record.

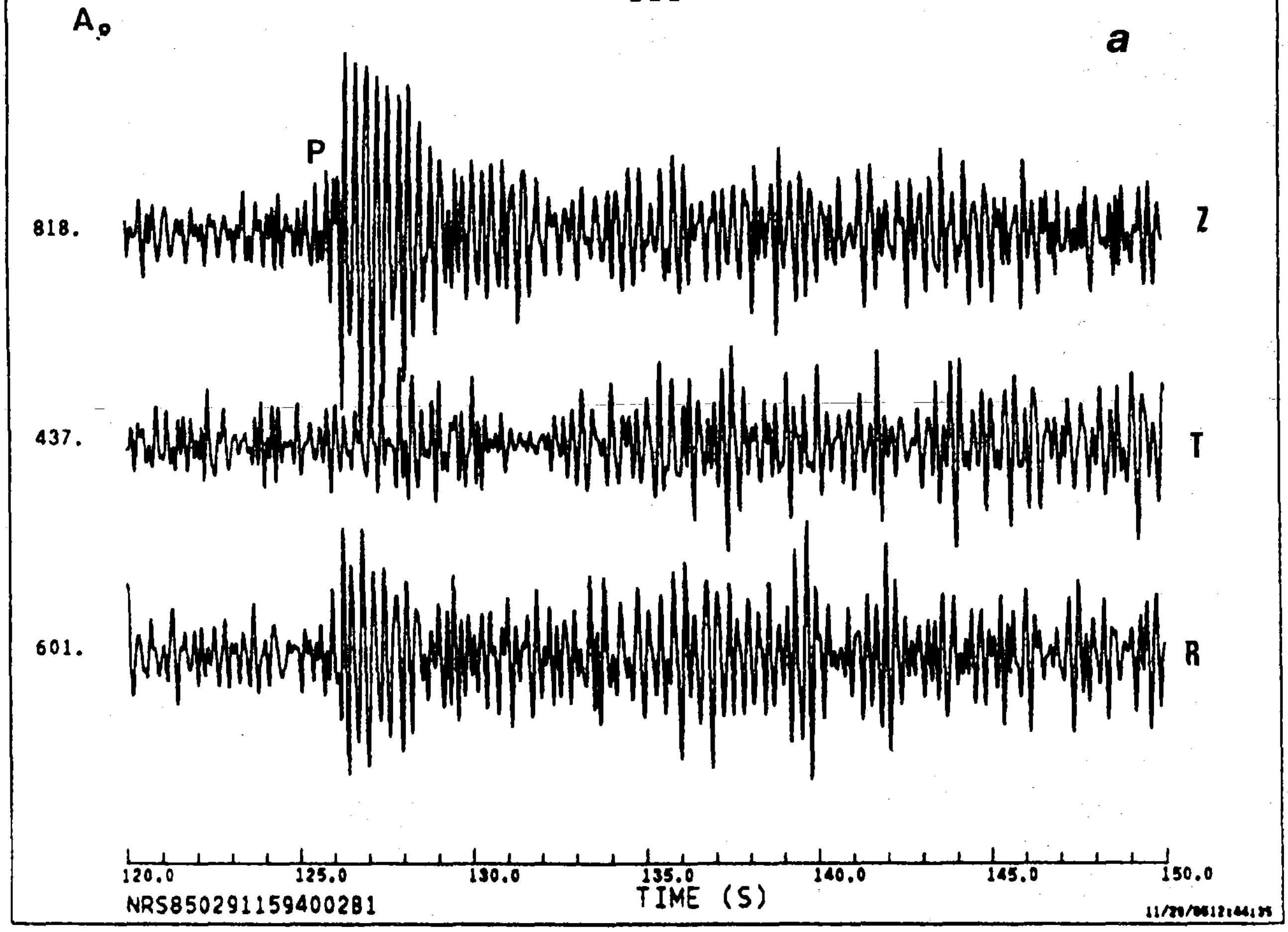

Ao
a
P
818.
Z
437.
T
601.
R
120.0
125.0
130.0
135.0
140.0
145.0
150.0
TIME (S)
NRS850291159400281

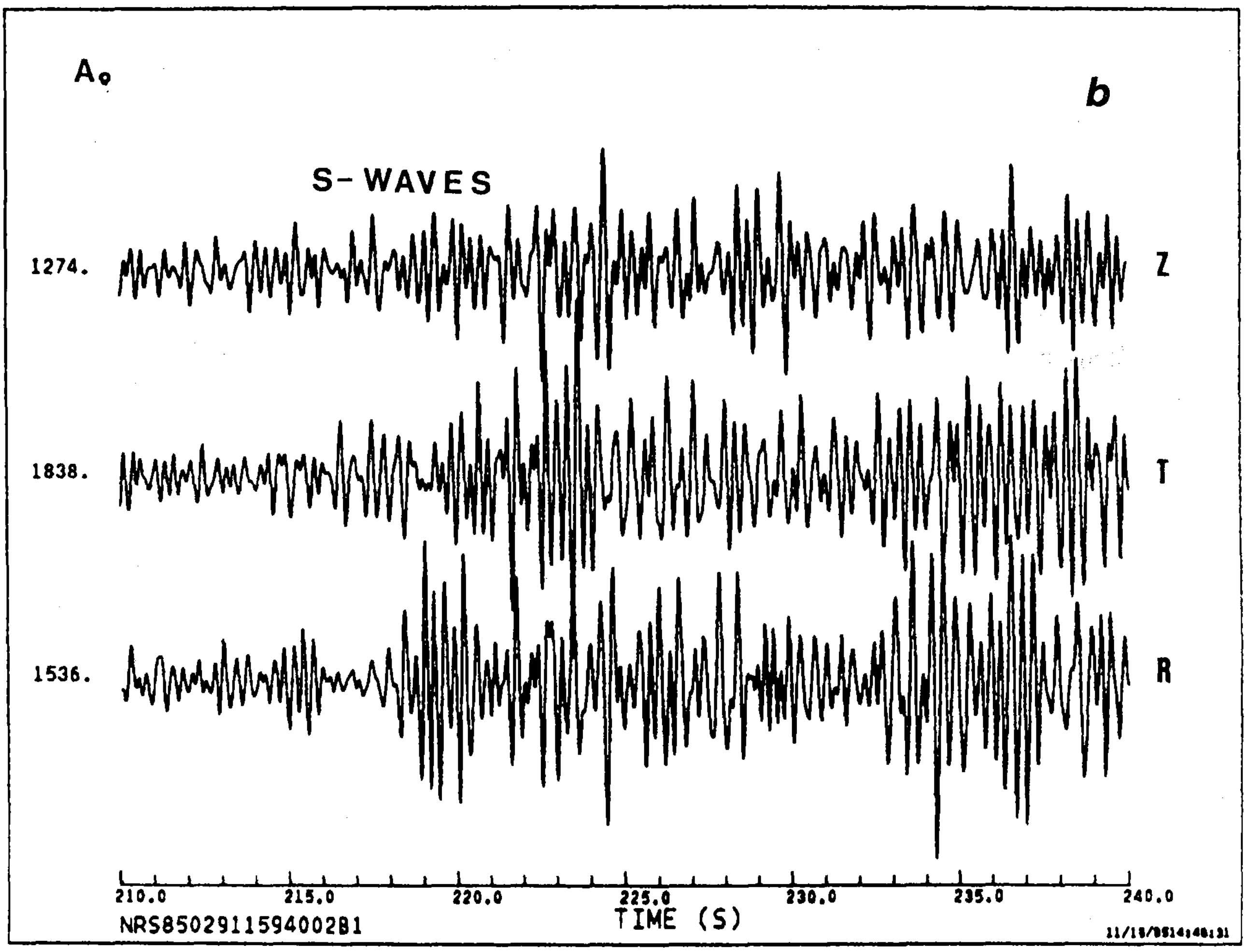

Ao
b
S- WAVES
1274.
Z
1838.
T
1536.
R
210.0
215.0
220.0
225.0
230.0
235.0
240.0
TIME (S)
NRS850291159400281

Fig. VII.9.1

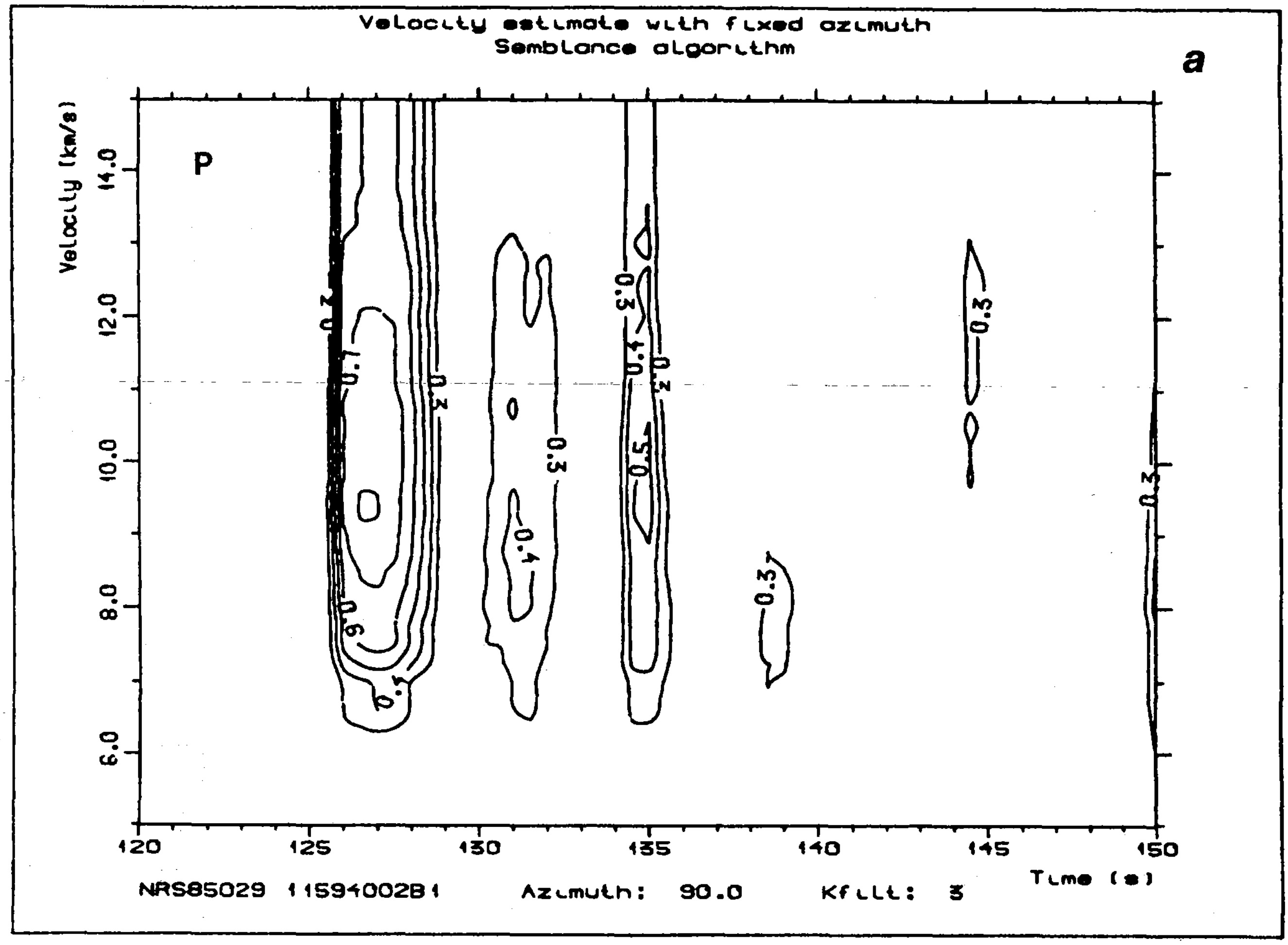
Velocity estimate with fixed azimuth
Semblance algorithm
a
Velocity (km/s)
P
Time (s)
NRS85029 11594002B1 Azimuth: 90.0 Kfilt: 3

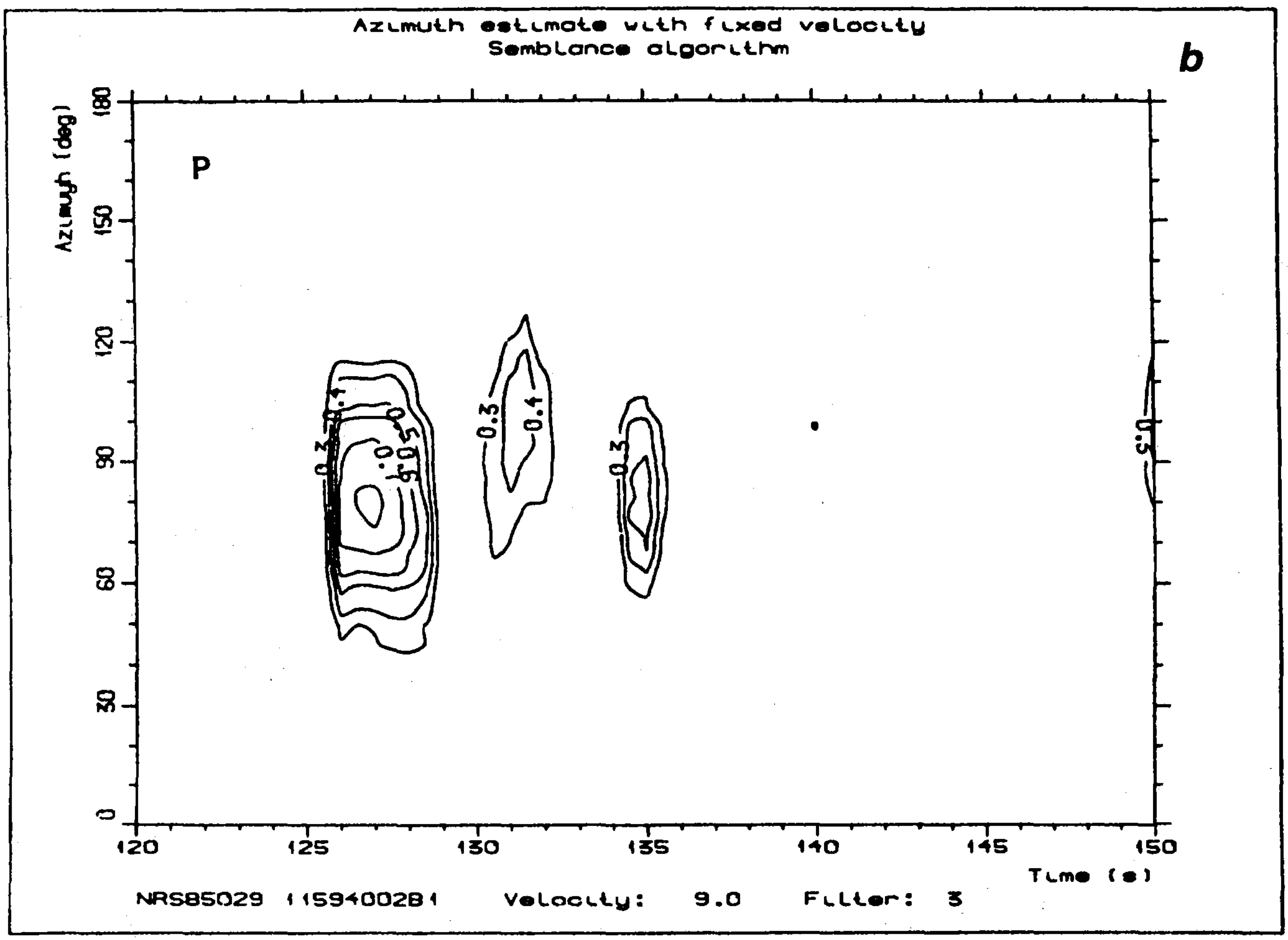
Azimuth estimate with fixed velocity
Semblance algorithm
b
Azimuth (deg)
P
Time (s)
NRS85029 11594002B1 Velocity: 9.0 Filter: 3

Fig. VII.9.2

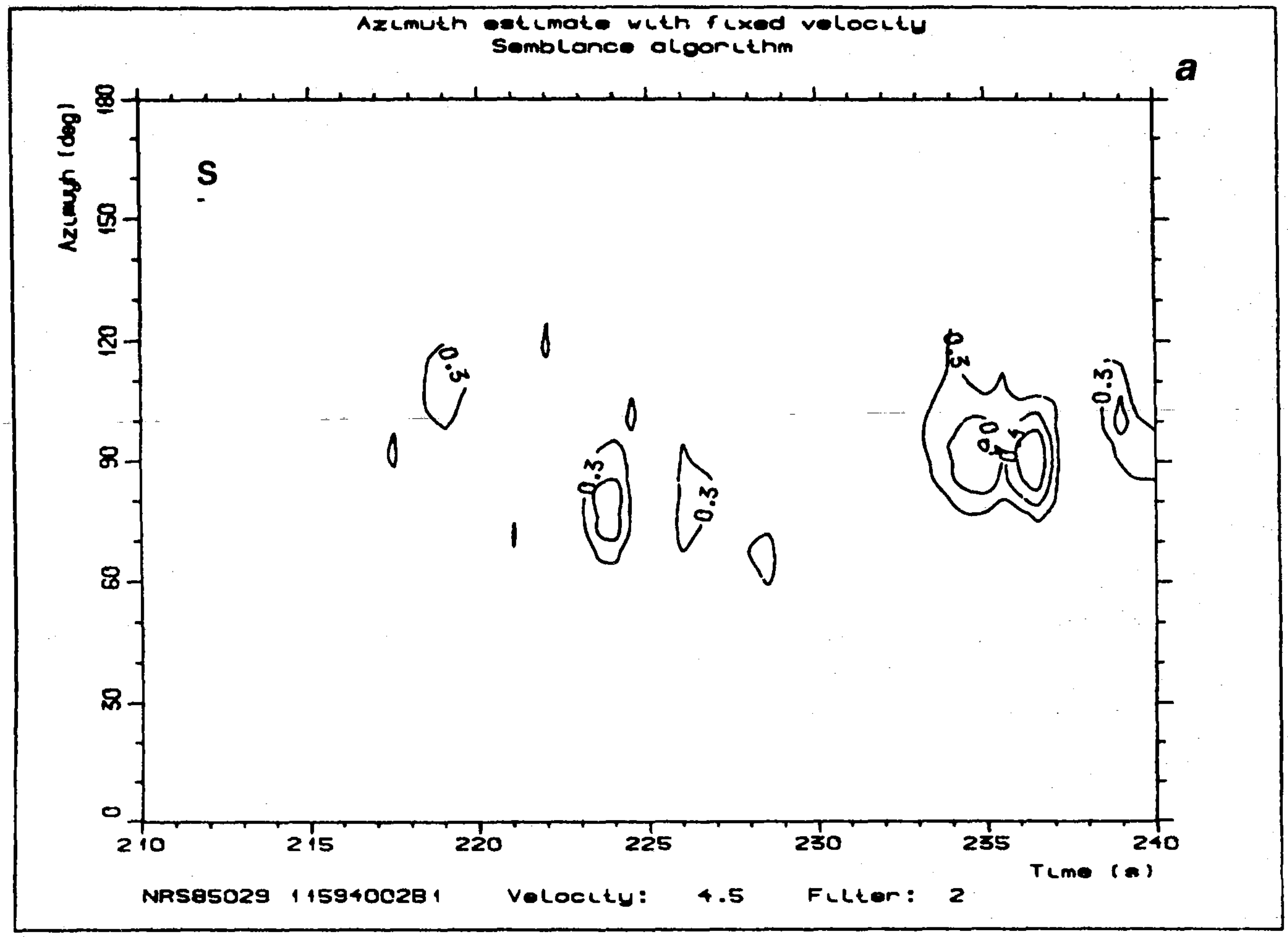
Azimuth estimate with fixed velocity
Semblance algorithm
a
Azimuth (deg)
S
0.3
Time (s)
NRS85029 11594002B1 Velocity: 4.5 Filter: 2

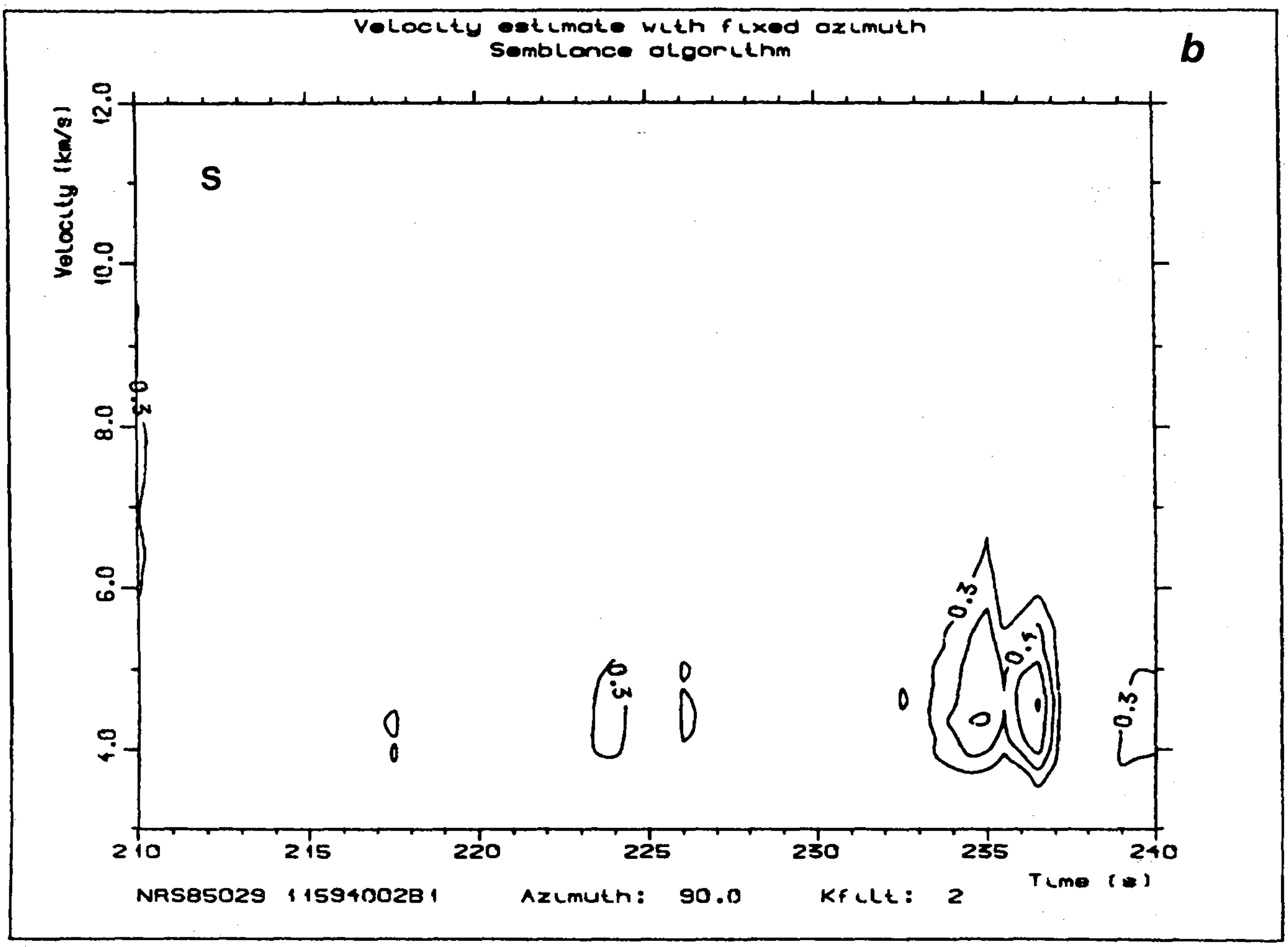
Velocity estimate with fixed azimuth
Semblance algorithm
b
Velocity (km/s)
S
0.3
Time (s)
NRS85029 11594002B1 Azimuth: 90.0 Kfilt: 2

Fig. VII.9.3

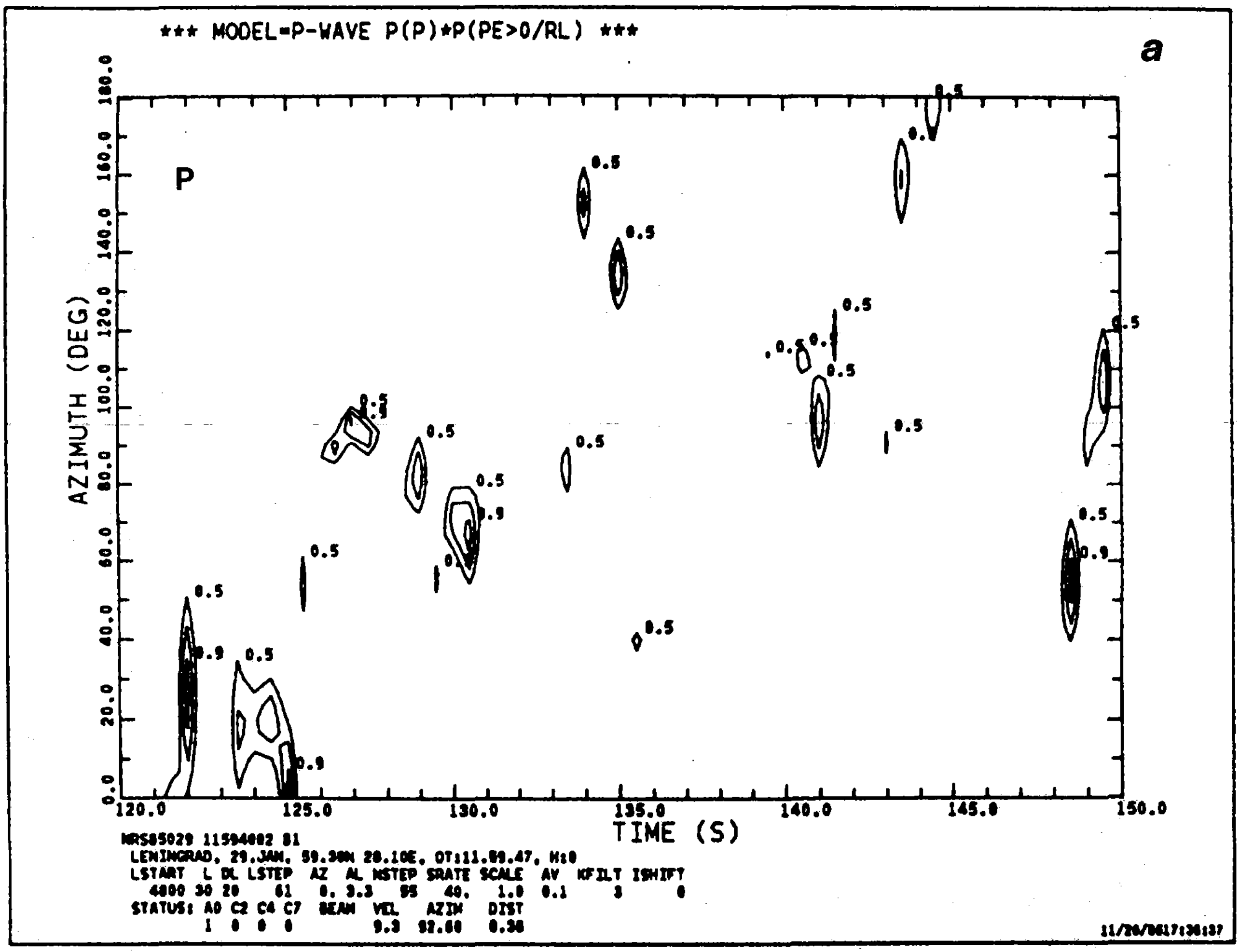
*** MODEL=P-WAVE P(P)*P(PE>0/RL) ***
a
P
AZIMUTH (DEG)
TIME (S)
NRS85029 11594002 81
LENINGRAD, 29.JAN, 59.30N 28.10E, OT:11.59.47, H:0
LSTART L DL LSTEP AZ AL NSTEP SRATE SCALE AV KFILT ISHIFT
4800 30 20 61 0. 3.3 55 40. 1.0 0.1 3 0
STATUS: A0 C2 C4 C7 BEAM VEL AZIM DIST
1 0 0 0 9.3 92.60 0.38

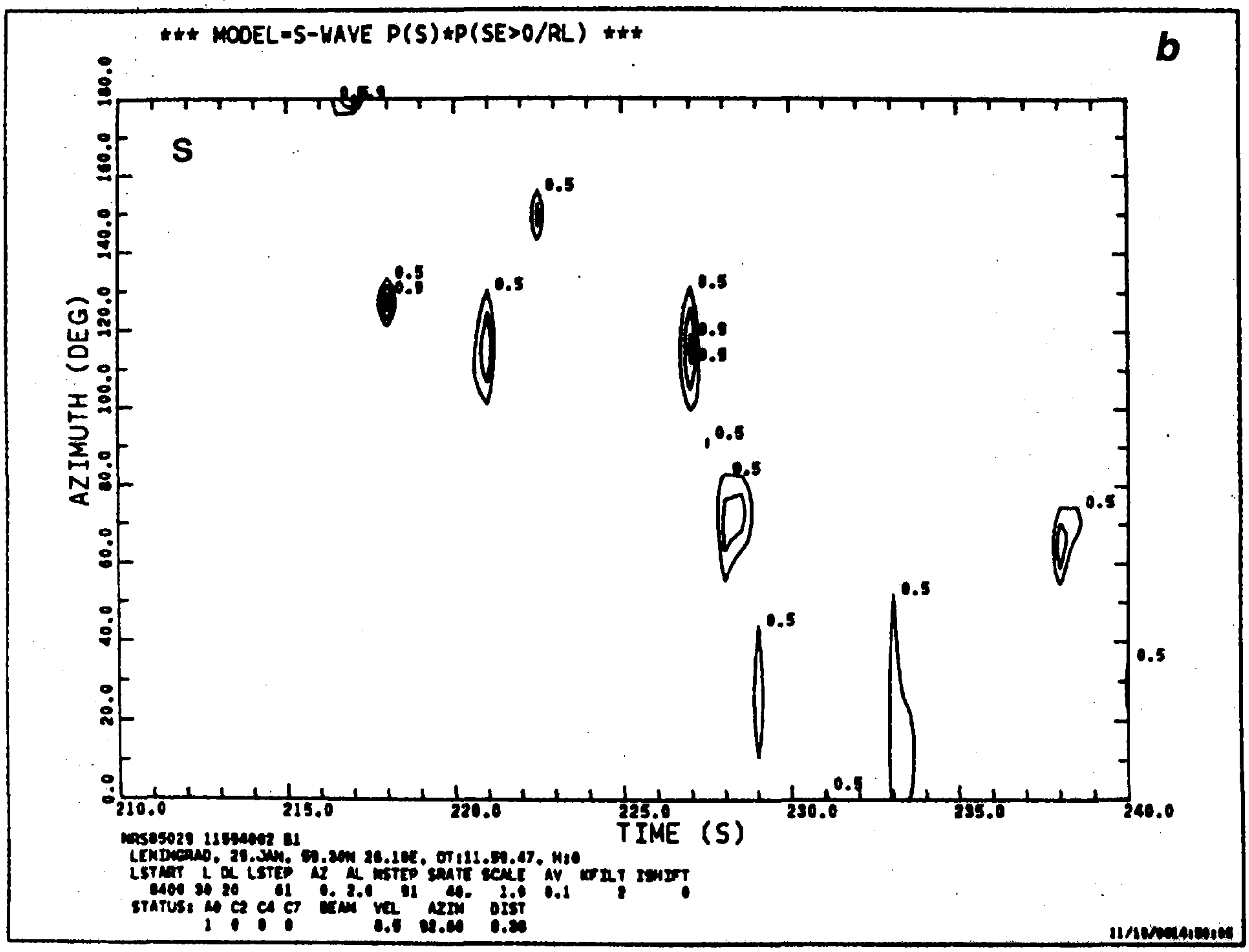
*** MODEL=S-WAVE P(S)*P(SE>0/RL) ***
b
S
AZIMUTH (DEG)
TIME (S)
NRS85029 11594002 81
LENINGRAD, 29.JAN, 59.30N 28.10E, OT:11.59.47, H:0
LSTART L DL LSTEP AZ AL NSTEP SRATE SCALE AV KFILT ISHIFT
8400 30 20 61 0. 2.0 91 40. 1.0 0.1 2 0
STATUS: A0 C2 C4 C7 BEAM VEL AZIM DIST

Fig. VII.9.4

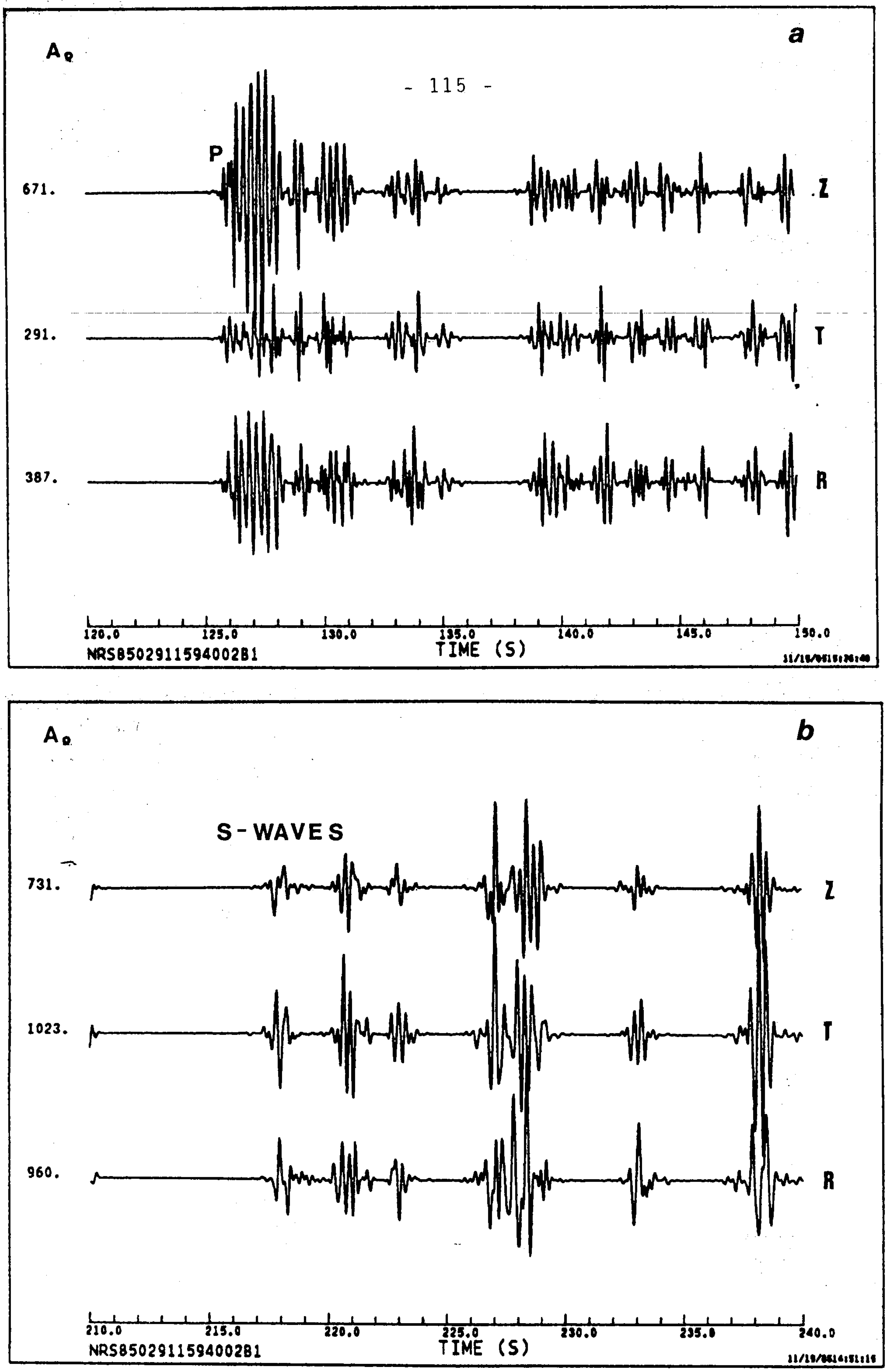
a
P
671.
291.
387.
Z
T
R
120.0
125.0
130.0
135.0
140.0
145.0
150.0
TIME (S)
NRS8502911594002B1
b
S-WAVES
731.
1023.
960.
Z
T
R
210.0
215.0
220.0
225.0
230.0
235.0
240.0
TIME (S)
NRS8502911594002B1

Fig. VII.9.5

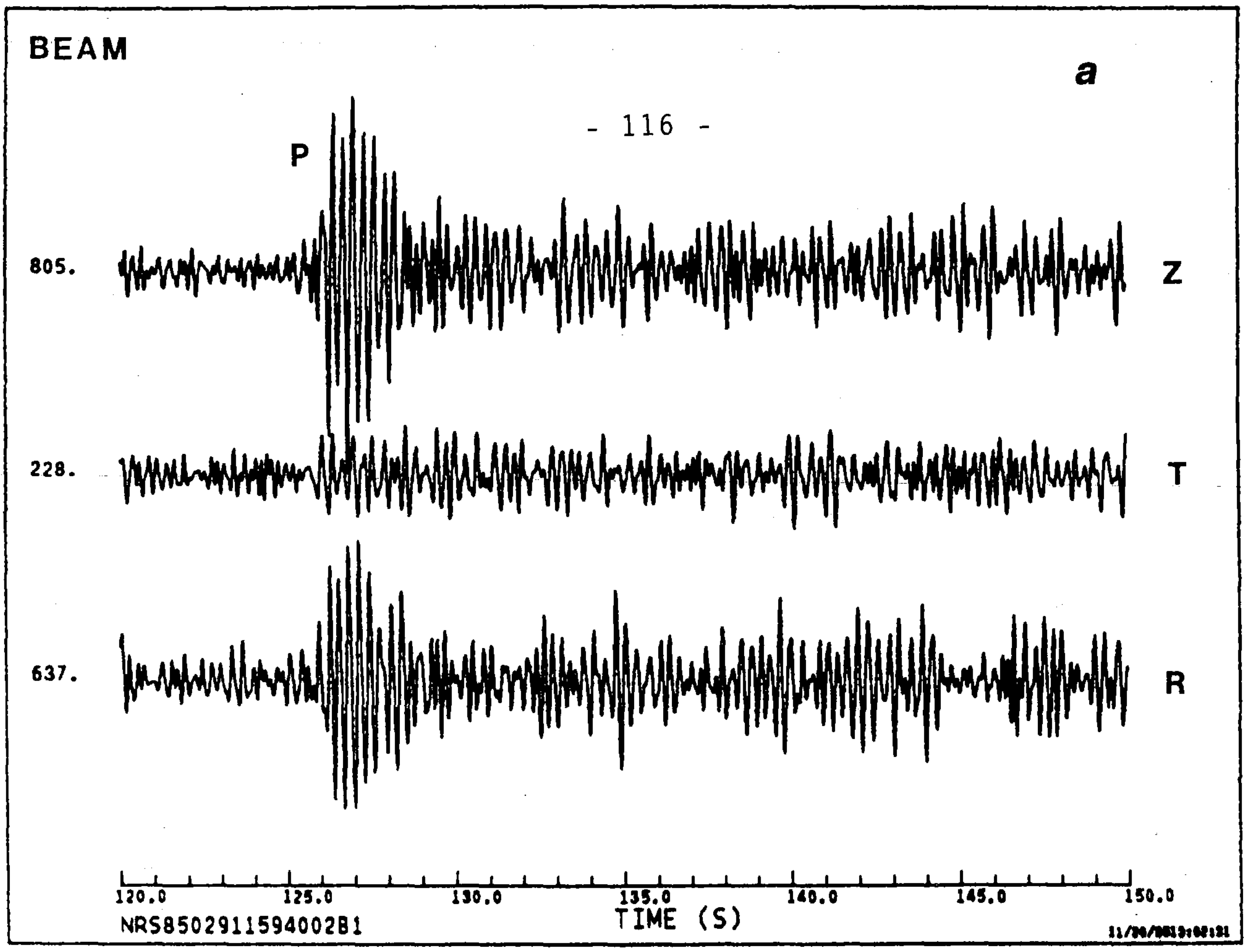
BEAM
a
P
805.
Z
228.
T
637.
R
120.0
125.0
130.0
135.0
140.0
145.0
150.0
TIME (S)
NRS8502911594002B1

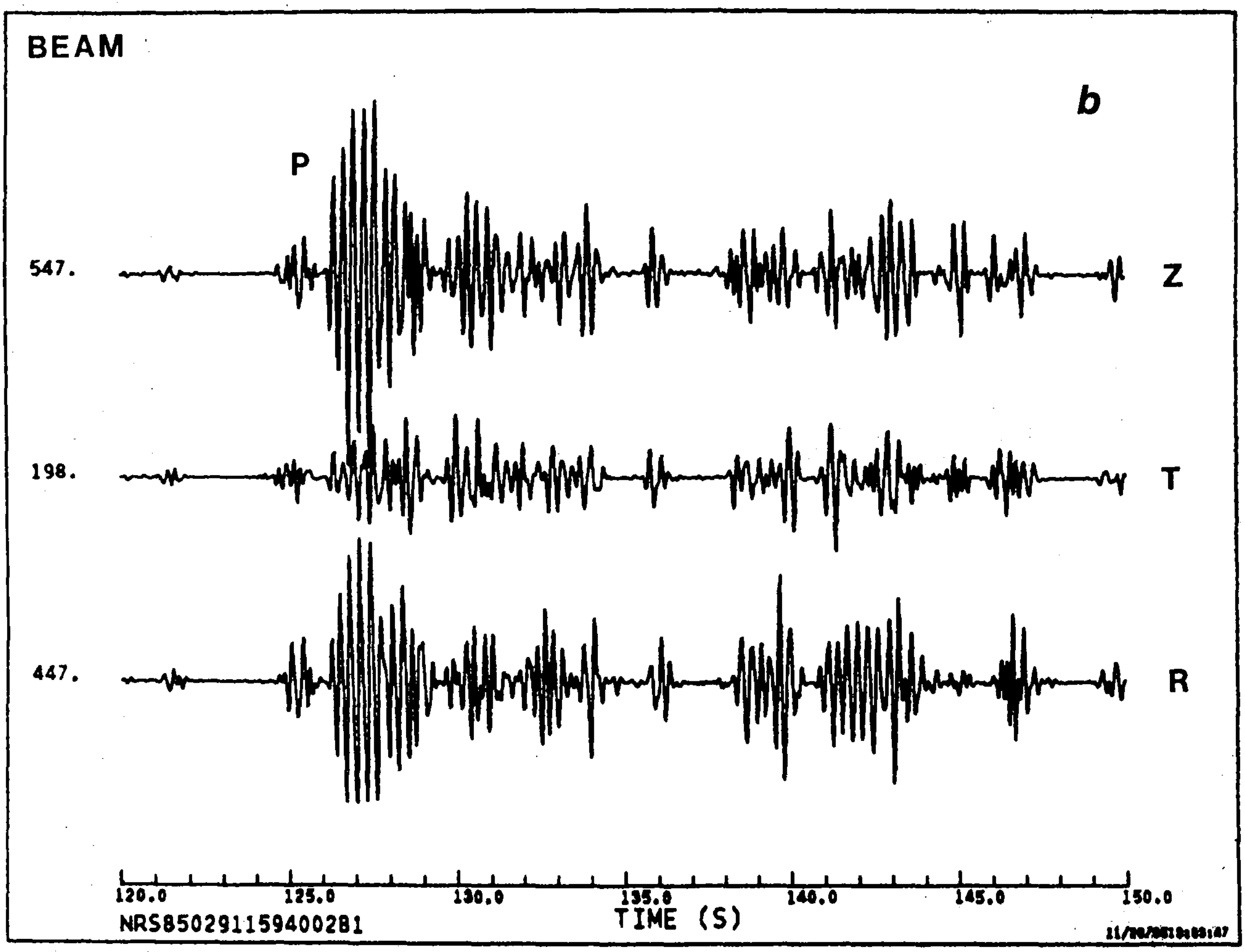
BEAM
b
P
547.
Z
198.
T
447.
R
120.0
125.0
130.0
135.0
140.0
145.0
150.0
TIME (S)
NRS8502911594002B1

Fig. VII.9.6

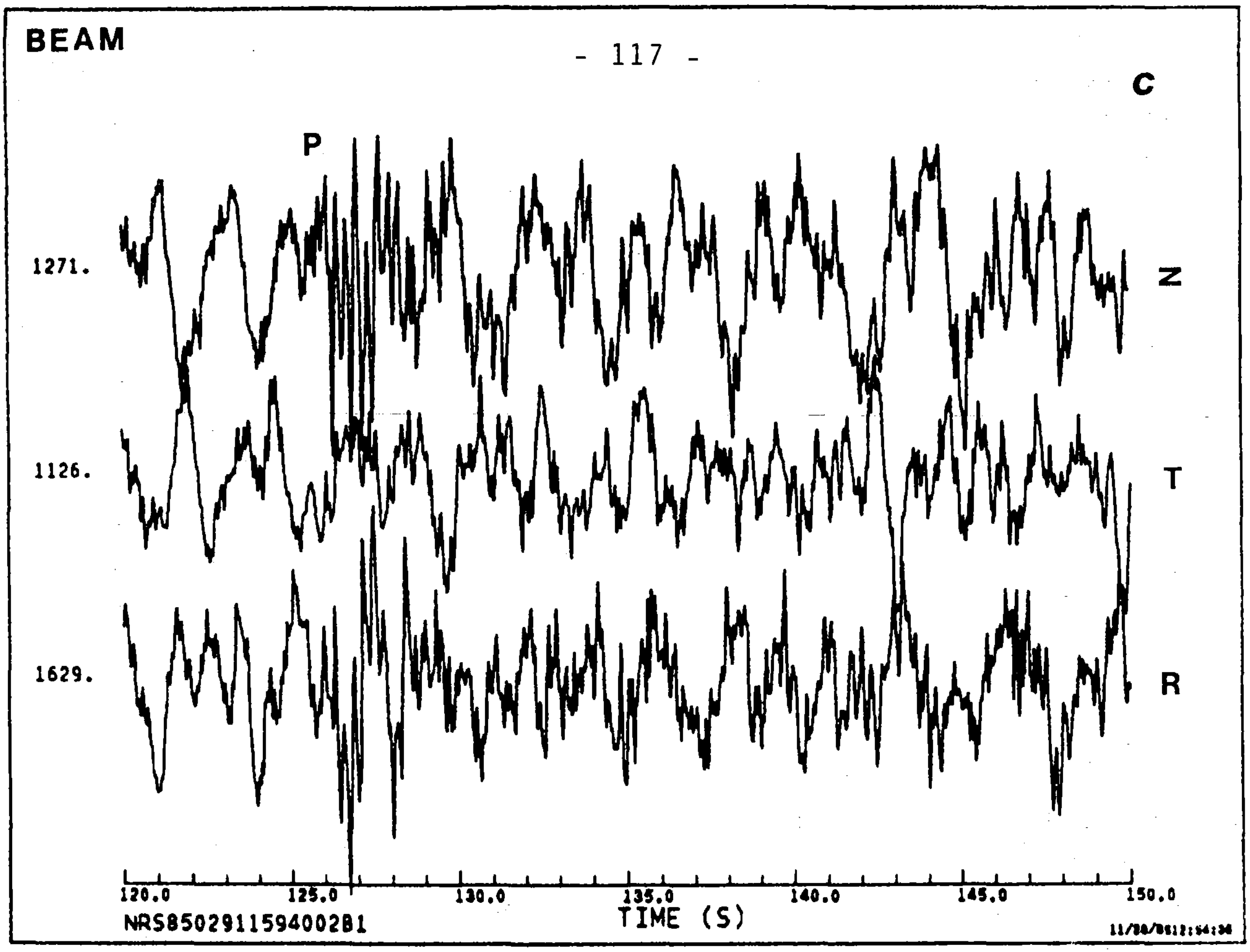

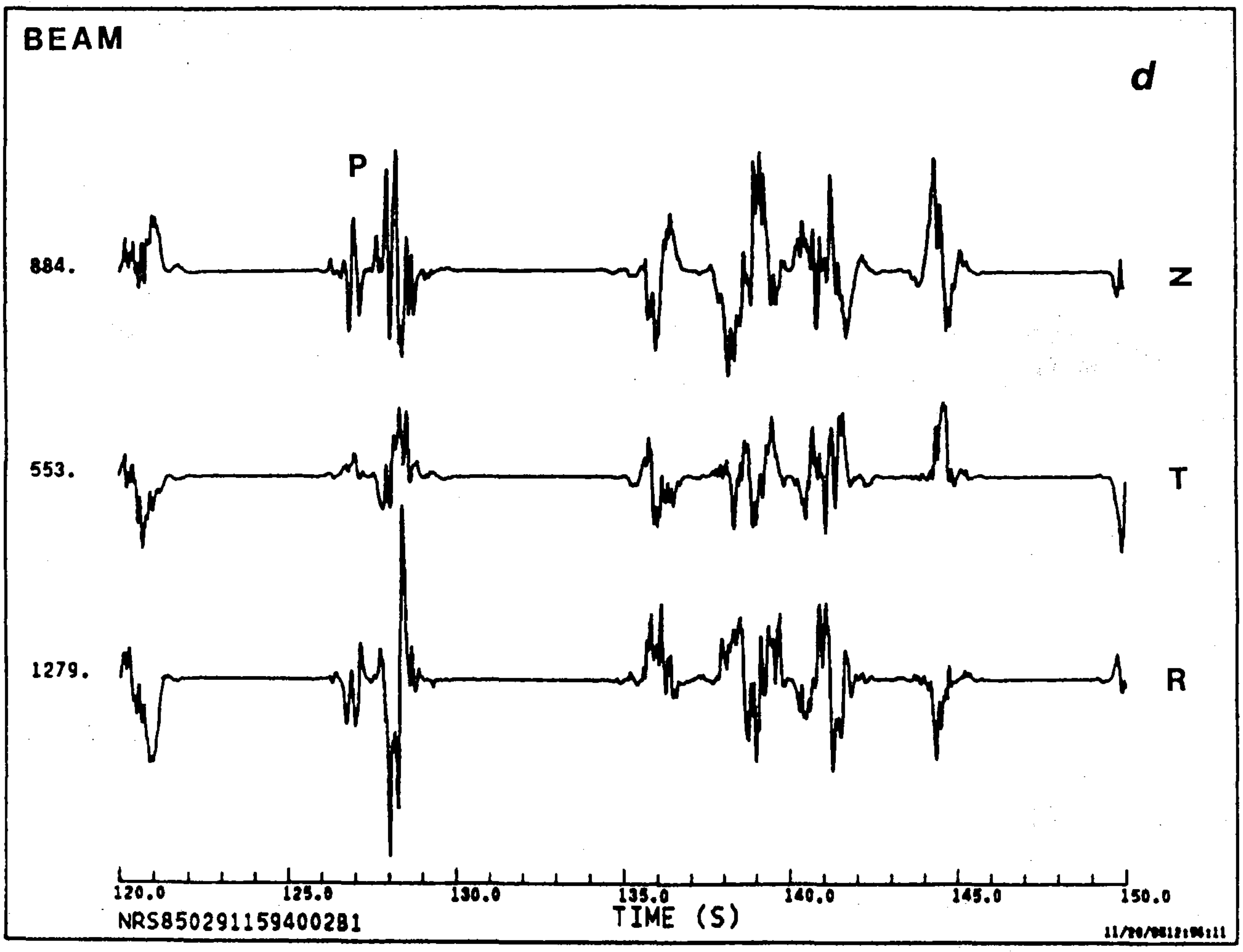

Fig. VII.9.6 (cont.)

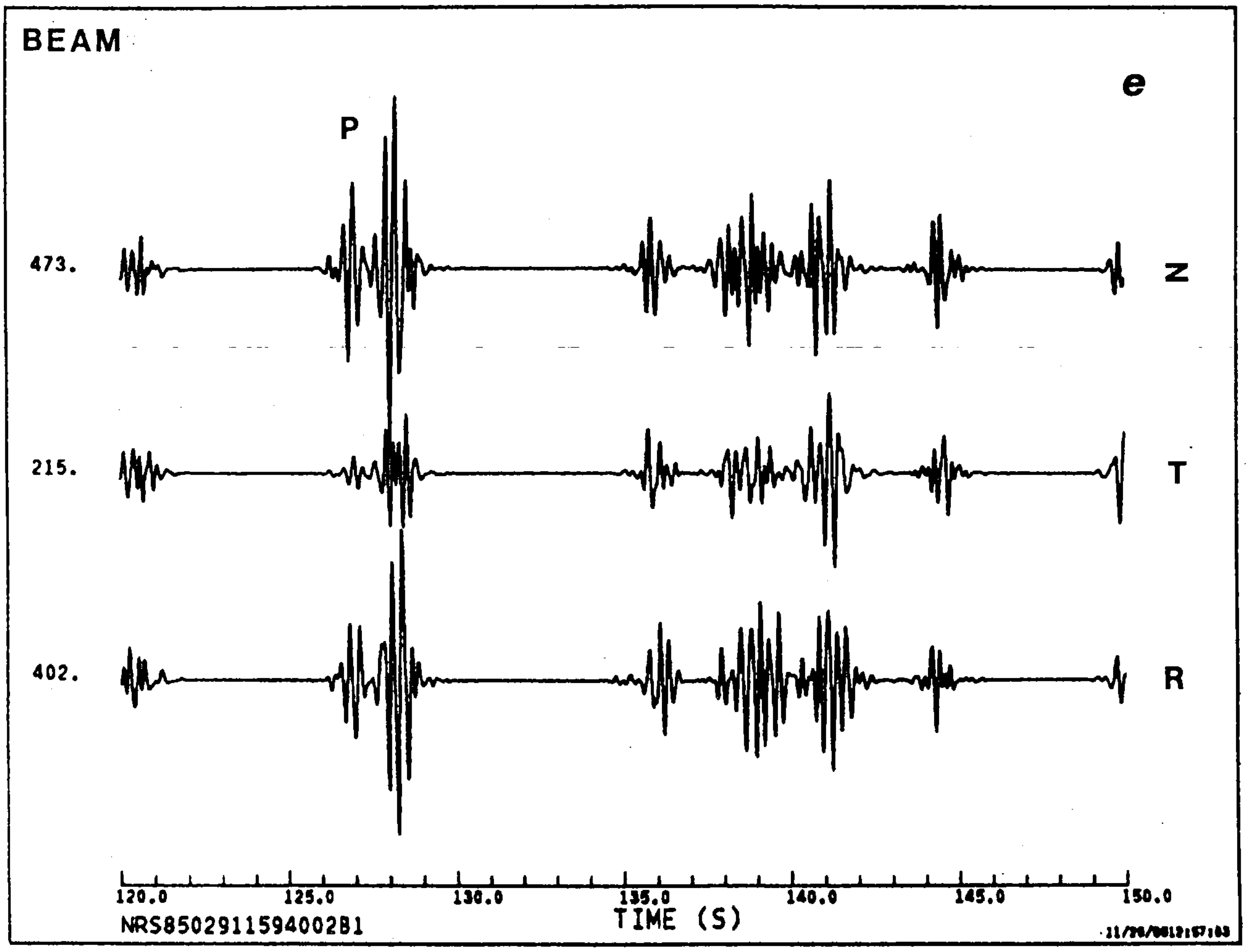

Fig. VII.9.6 (cont.)